

Supporting information

Facile synthesis of shape-stable phase-change composites via adsorption of stearic acid onto cellulose microfibers

Denis V. Voronin^{*1,2}, Rais I. Mendgaziev¹, Maria I. Rubtsova¹, Kirill A. Cherednichenko¹, Polina A. Demina², Anna M. Abramova², Dmitry G. Shchukin³, and Vladimir Vinokurov¹

1 National University of Oil and Gas «Gubkin University», Moscow 119991, Russia

2 Saratov State University, Saratov 410012, Russia

3 Stephenson Institute for Renewable Energy, Department of Chemistry, University of Liverpool, Liverpool L69 7ZD, United Kingdom

*E-mail: denis.v.voronin@gmail.com

Confocal laser scanning microscopy (CLSM) study of the distribution of stearic acid (SA) mixed with the Nile Red (NR) dye on the surface of cellulose microfibers (MFC)

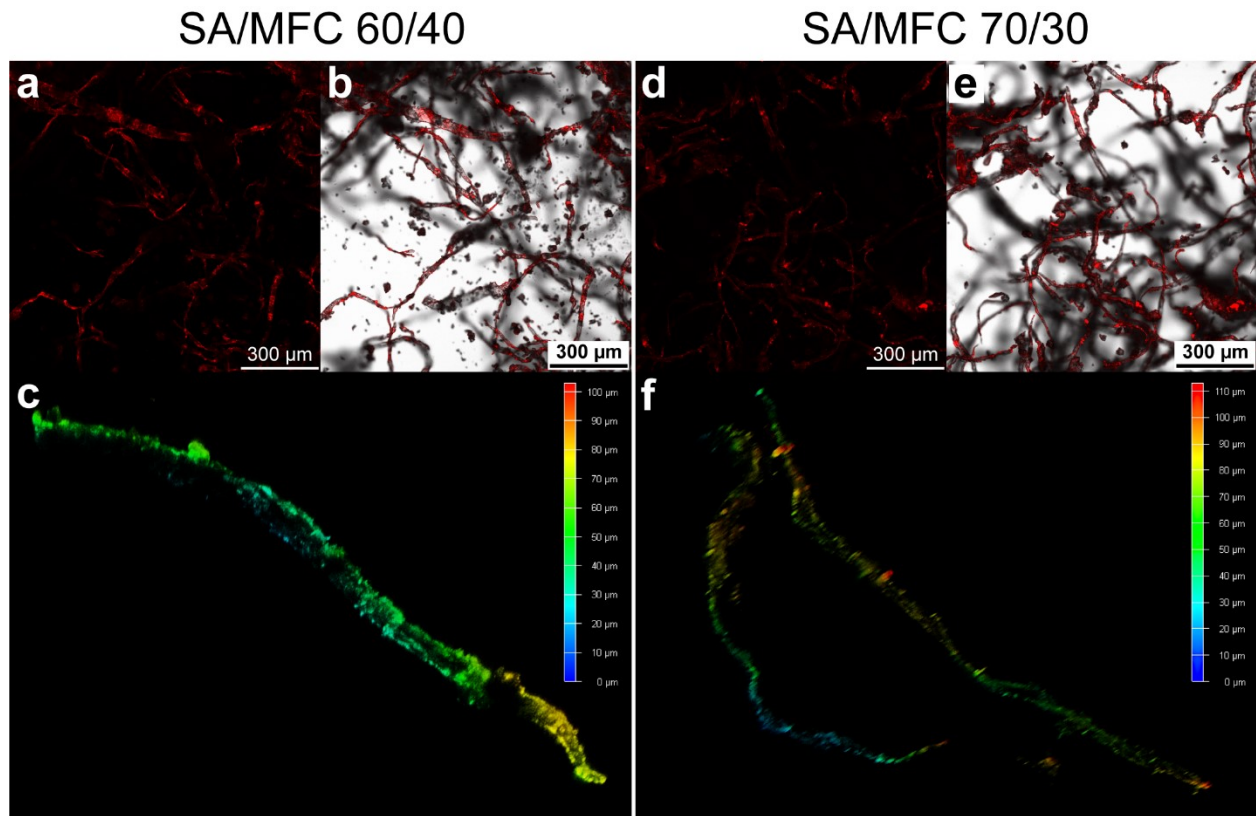


Figure S1. CLSM images of the SA/MFC 60/40 (a-c) and SA/MFC 70/30 (d-f) composite fibers showing the distribution of Nile Red labeled SA onto the MFC surface: (a) and (d) are fluorescent CLSM images; (b) and (e) are merged fluorescent and transmittance CLSM images; (c) and (f) are 3D reconstructed fluorescent CLSM images.

The distribution of the SA mixed with Nile Red dye on the surface of the cellulose microfibers was studied with CLSM measurements. Figure S1a and Figure S2d show the fluorescent images of the SA/MFC fibers captured under excitation by a 515 nm laser. The fluorescent emission follows the shape of the cellulose microfibers that is also seen on the merged fluorescent and transmission images (Figure S1b and Figure S1e). The 3D images of the single fibers demonstrate the uniform coating of MFC with SA, which is following the bending of the fibers as it is shown by the color depth coding (Figure S1c and Figure S1d). Some pieces of the free-standing SA can be seen on the transmission images as well.

The assignment of absorption bands in the FTIR spectra of MFC and SA

Table S1. The assignment of absorption bands in the FTIR spectra of MFC and SA

Wavenumber, cm ⁻¹	Assignment		Strength	Reference
	MFC	SA		
688	-	O=C=O in-plane deformation	m	[1]
722	-	CH ₂ rock	vs	[1]
896	Glucose ring deformation	-	np	[2, 3]
940	-	C–OH out-of-plane deformation	np	[1]
1036	C–O stretching	-	np	[2, 3]
1057	C–O stretching	-	np	[2, 3]
1108	Glucose ring antisymmetric stretching	-	np	[2, 3]
1162	C–O–C antisymmetric vibration	-	np	[2, 3]
1297	-	C–OH stretching	s	[1]
1430	-	C–OH in-plane bending	m	[1]
1462	-	CH ₂ scissor	s	[1]
1700	-	C=O stretching	vs	[1]
2700 – 3000	CH stretching	-	np	[2, 3]
2848	-	CH ₂ symmetric stretching	vs	[1]
2915	CH ₂ antisymmetric stretching	CH ₂ antisymmetric stretching	np/vs	[1]
2953	-	CH ₃ antisymmetric stretching	m	[1]
2500 – 3500	-	OH stretching vibrations in carboxyl group	w	[1]
3050 – 3600	Stretching of OH groups involved into intermolecular	-	np	[2, 3]

	interactions via hydrogen bonding			
Abbreviations: s=strong; m=medium; w=weak; v=very; np=not present; MFC=microfibrillar cellulose; SA=stearic acid.				

Melting points, freezing points, loading efficiency, and thermal storage capability of SA/MFC composites figured out from the DSC data

Table S2. The summary of thermal properties of SA and SA/MFC composites measured by DSC

Sample	T_M , °C	ΔH_M , J/g	T_F , °C	ΔH_F , J/g	E, %	η , %
SA	61	178	51	182	-	-
SA/MFC 70/30	61	125	51	125	69	99
SA/MFC 65/35	62	120	50	123	66	99
SA/MFC 60/40	61	107	51	106	59	98

Table S3. Melting and freezing points of SA/MFC composites measured during thermal reliability evaluation

Sample	T_M , °C					T_F , °C				
	1	5	10	15	20	1	5	10	15	20
SA/MFC 70/30	61	62	62	62	62	51	50	50	50	50
SA/MFC 65/35	62°	62	62	62	62	50	50	50	50	50
SA/MFC 60/40	61	61	61	61	61	51	51	51	51	51

Table S4. The melting and freezing enthalpies of the SA/MFC composites calculated from the thermal reliability data measured with DSC

Sample	ΔH_M , J/g					ΔH_F , J/g				
	1	5	10	15	20	1	5	10	15	20
SA/MFC 70/30	125	123	123	123	123	125	125	125	125	125
SA/MFC 65/35	120	118	118	118	118	123	120	120	120	120
SA/MFC 60/40	107	107	105	105	105	106	107	107	108	108

Table S5. Loading efficiency (E), and thermal storage capability (η) of SA/MFC composites calculated from the thermal reliability data measured with DSC

Sample	$E, \%$					$\eta, \%$				
	1	5	10	15	20	1	5	10	15	20
SA/MFC 70/30	69	69	69	69	69	99	99	99	99	99
SA/MFC 65/35	66	66	66	66	66	99	99	99	99	99
SA/MFC 60/40	59	59	59	59	59	98	98	99	99	99

Comparison of thermal stability of MFC, SA, and SA/MFC composites**Table S6.** Thermal stability properties of MFC, SA, and SA/MFC composites measured with TGA

<i>Sample</i>	<i>T_{on}, °C</i>	<i>MRDT, °C</i>	<i>Residue, %</i>
MFC	289	327	1
		456	
SA	246	272	2
		218	
		329	
SA/MFC 70/30	191	459	4
		222	
		327	
		454	
SA/MFC 65/35	193	215	1
		329	
		453	
SA/MFC 60/40	187	215	1
		329	
		453	

Confocal laser scanning microscopy images of SA/MFC 60/40 and SA/MFC 70/30 composites after heating at 75°C and 120°C

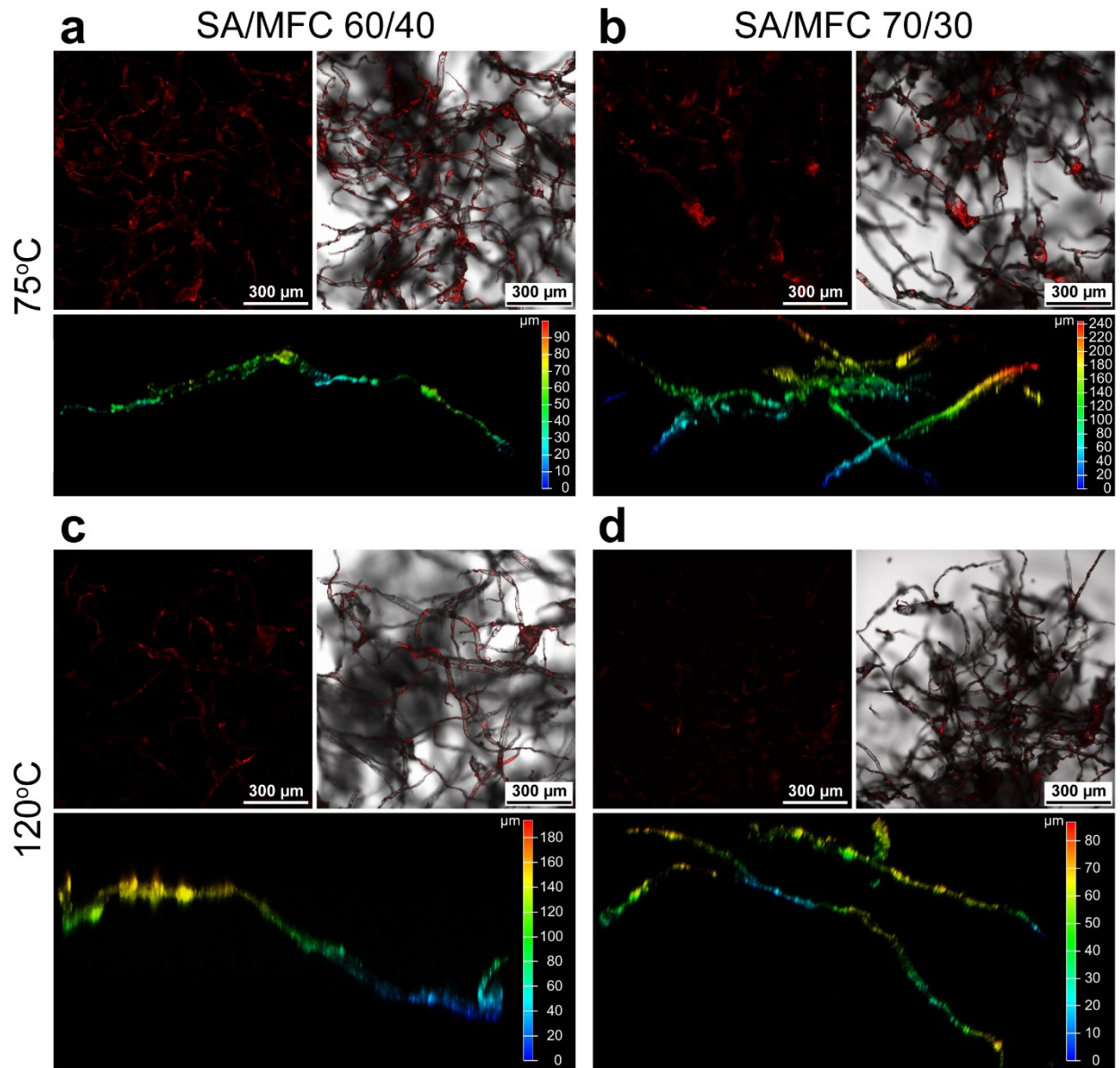


Figure S2. CLSM images of SA/MFC 60/40 and SA/MFC 70/30 composites after 5 heating cycles at 75°C (a, b) and 120°C (c, d).

FTIR spectra of SA/MFC 60/40 and SA/MFC 70/30 composites before and after heating at 75°C and 120°C

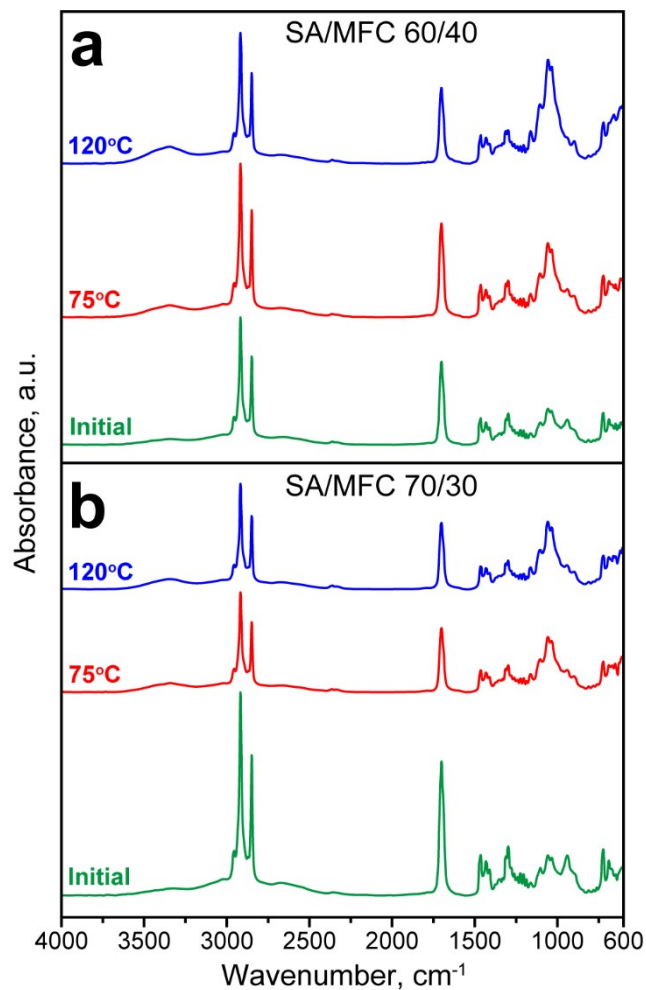


Figure S3. FTIR spectra of SA/MFC 60/40 (a) and SA/MFC 70/30 (b) composites before and after heating at 75°C and 120°C.

Latent heat storage/release properties of SA/MFC composites after 20 heating cycles at 75°C and 120°C

Table S7. Summary of the thermal properties of SA/MFC 60/40 and SA/MFC 70/30 composites before and after the material leakage test

Sample	T_M , °C	ΔH_M , J/g	T_F , °C	ΔH_F , J/g	E , %	η , %
<i>Initial</i>						
SA/MFC 70/30	61	125	51	125	69	99
SA/MFC 60/40	61	107	51	106	59	98
<i>20 heating cycles at 75°C</i>						
SA/MFC 70/30	63	122	49	123	68	99
SA/MFC 60/40	62	107	50	109	60	98
<i>20 heating cycles at 120°C</i>						
SA/MFC 70/30	64	114	50	116	64	99
SA/MFC 60/40	64	87	54	91	49	99

References

- [1] Pudney PDA, Mutch KJ, Zhu S. Characterising the phase behaviour of stearic acid and its triethanolamine soap and acid-soap by infrared spectroscopy. *Phys Chem Chem Phys.* 2009;11(25):5010-8. <https://dx.doi.org/10.1039/B819582J>.
- [2] Pandey KK. A study of chemical structure of soft and hardwood and wood polymers by FTIR spectroscopy. *J Appl Polym Sci.* 1999;71(12):1969-75. [https://dx.doi.org/10.1002/\(sici\)1097-4628\(19990321\)71:12<1969::aid-app6>3.0.co;2-d](https://dx.doi.org/10.1002/(sici)1097-4628(19990321)71:12<1969::aid-app6>3.0.co;2-d).
- [3] Makarem M, Lee CM, Kafle K, Huang S, Chae I, Yang H, et al. Probing cellulose structures with vibrational spectroscopy. *Cellulose.* 2019;26(1):35-79. <https://dx.doi.org/10.1007/s10570-018-2199-z>.